



HAL
open science

(Finite) statistical size effects on compressive strength

Jérôme Weiss, Lucas Girard, Florent Gimbert, David Amitrano, Damien Vandembroucq

► **To cite this version:**

Jérôme Weiss, Lucas Girard, Florent Gimbert, David Amitrano, Damien Vandembroucq. (Finite) statistical size effects on compressive strength. Proceedings of the National Academy of Sciences of the United States of America, 2014, pp.201403500. 10.1073/pnas.1403500111 . hal-00989386

HAL Id: hal-00989386

<https://hal.science/hal-00989386>

Submitted on 11 May 2014

HAL is a multi-disciplinary open access archive for the deposit and dissemination of scientific research documents, whether they are published or not. The documents may come from teaching and research institutions in France or abroad, or from public or private research centers.

L'archive ouverte pluridisciplinaire **HAL**, est destinée au dépôt et à la diffusion de documents scientifiques de niveau recherche, publiés ou non, émanant des établissements d'enseignement et de recherche français ou étrangers, des laboratoires publics ou privés.

(Finite) statistical size effects on compressive strength

Jérôme Weiss^{1,*}, Lucas Girard², Florent Gimbert^{3,4}, David Amitrano⁴ and Damien Vandembroucq⁵

¹Laboratoire de Glaciologie et Géophysique de l'Environnement, CNRS/Université J. Fourier, 54 Rue Molière, BP 96, 38402 St Martin d'Hères cedex, France

²School of Architecture, Civil and Environmental Engineering, Ecole Polytechnique Fédérale de Lausanne, EPFL ENAC IIE CRYOS, Switzerland

³California Institute of technology, Division of Geological and Planetary Sciences, Pasadena, CA 91125, USA

⁴Institut des Sciences de la Terre, CNRS/Université J. Fourier, 1381 Rue de la piscine, BP53, 38041 Grenoble cedex 9, France

⁵Laboratoire PMMH, UMR 7636 CNRS/ESPCI/Univ. Paris 6 UPMC/Univ. Paris 7 Diderot, 10 rue Vauquelin, 75231 Paris cedex 05, France

* Corresponding author: jerome.weiss@ujf-grenoble.fr

Abstract

The larger the structures, the lower their mechanical strength. Already discussed by da Vinci and Mariotte several centuries ago, size effects on strength remain of crucial importance in modern engineering for the elaboration of safety regulations in structural design, or the extrapolation of laboratory results to geophysical field scales. Under tensile loading, statistical size effects are traditionally modeled with a weakest link approach. One of its prominent results is a prediction of vanishing strength at large scales that can be quantified in the framework of extreme value statistics. Despite a frequent use outside its range of validity, this approach remains the dominant tool in the field of statistical size effects. Here we focus on compressive failure, which concerns a wide range of geophysical and geotechnical situations. We show on historical and recent experimental data that weakest link predictions are not obeyed. In particular, the mechanical strength saturates at a non-zero value towards large scales. Accounting explicitly for the elastic interactions between defects during the damage process, we build a formal analogy of compressive failure with the depinning transition of an elastic manifold. This critical transition interpretation naturally entails finite-size scaling laws for the mean strength and its associated variability. Theoretical predictions are in remarkable agreement with measurements reported for various materials such as rocks, ice, coal, or concrete. This formalism, which can also be extended to the flowing instability of granular media under multiaxial compression, has important practical consequences for future design rules.

Keywords

Mechanical strength; size-effect; compressive failure; critical transition; depinning

Significance statement

Large structures generally fail under stresses significantly lower than small ones. This is the size effect on strength, one of the oldest problems of engineering, already discussed by Leonardo da Vinci and Edmé Mariotte centuries ago. One classical explanation is the weakest link hypothesis: the largest the “chain”, the larger the probability to find a weak link whose breaking will set the failure of the whole chain. We show, however, that it is irrelevant in case of compressive loading, a situation particularly crucial for e.g. geotechnical problems. Interpreting compressive failure as a critical transition between an “intact” and a “failed” state, we quantitatively explain the size effects on compressive strength of materials such as concrete, rocks, coal, ice, or granular materials.

\body

Introduction

Owing to its importance for structural design(1), the elaboration of safety regulations(2), or the extrapolation of laboratory results to geophysical field scales(3), the size effects on strength of materials is one of the oldest problems in engineering, already discussed by Leonardo da Vinci and Edmé Mariotte(4) several centuries ago, but still an active field of research(5, 6). As early as 1686, Mariotte(4) qualitatively introduced the weakest-link concept to account for size effects on mechanical strength, a phenomenon evidenced by Leonardo da Vinci almost two centuries earlier. This idea, which states that the larger the system considered, the larger the probability to find a particularly faulty place that will be at the origin of global failure, was formalized much later by Weibull(7). Considering a chain of elementary independent links, the failure of the chain is obtained as soon as one link happens to break. By virtue of the independence between the potential breaking events, the survival probability of a chain of N links is obtained by the simple multiplication of the N elementary probabilities. Depending on the properties of the latter, the global survival probability converges toward one of the three limit distributions identified by Weibull, Gumbel(8) and Fréchet respectively. Together with Fisher and Tippett(9), these authors pioneered the field of extreme value statistics.

This purely statistical argument, undoubtedly valid in 1D, was extended by Weibull(7, 10) to account for the risk of failure of 3D samples or structures. Beside the hypothesis of independence, it thus requires an additional hypothesis of brittleness: the nucleation of any elementary crack at the microscopic scale from a pre-existing flaw is assumed to immediately induce the failure at the macro-scale. More specifically, following linear elastic fracture mechanics (LEFM) stating that crack initiation from a flaw of size s occurs at a stress $\sigma_c \sim s^{-1/2}$, one gets a probability of failure of a system of size L under an applied stress σ , $P_F(\sigma, L)$, that depends on the distribution of pre-existing defect sizes. Assuming a power law tail for this distribution, Weibull statistics are expected(7),

$$P_F(\sigma, L) = 1 - \exp\left(-\left(\frac{L}{L_0}\right)^d \left(\frac{\sigma}{\sigma_u}\right)^m\right),$$
 whereas Gumbel statistics are expected for any

distribution of defect sizes whose the tail falls faster than a power law (8, 11, 12),

$$P_f(\sigma, L) = 1 - \exp\left(-\left(\frac{L}{L_0}\right)^d \exp\left(\frac{\sigma}{\sigma_u}\right)\right),$$

where m is the so-called Weibull's modulus, d is the topological dimension and L_0 and σ_u are normalizing constants. For Weibull statistics, the mean strength $\langle\sigma_f\rangle$ and the associated standard deviation $\delta(\sigma_f)$ then scale with sample size L as $\langle\sigma_f\rangle(L) \sim \delta(\sigma_f)(L) \sim L^{-d/m}$. This approach has been successfully applied to the statistics of brittle failure strength under tension(7, 13), with m in the range 6 to 30(14). It implies a vanishing strength for $L \rightarrow +\infty$, although this decrease can be rather shallow, owing to the large values of m often reported.

Although relying on strong hypotheses, this weakest-link statistical approach was almost systematically invoked until the 70's to account for size effects on strength whatever the material and/or the loading conditions. However, as shown by Bažant(1, 5), in many situations the hypothesis of brittleness is not obeyed. This is in particular the case when the size of the fracture process zone (FPZ) becomes non-negligible with respect to the system size. In this so-called quasi-brittle case, an energetic, non-statistical size effect applies(15), which has been shown to account for a large variety of situations (5). Towards large scales, i.e. $L \rightarrow +\infty$, the FPZ becomes negligible compared to L , the hypothesis of brittleness should therefore be recovered and statistical size effects should dominate. Statistical numerical models of fracture of heterogeneous media also revealed deviations from the extreme value statistics predictions(16) but, as stated by Alava et al. (11), "the role of damage accumulation for fracture size effects in unnotched samples still remains unclear". As shown below, compressive failure results from such progressive damage accumulation.

In what follows, we do not consider (deterministic) energetic size effects and explore a situation, compressive failure, where both the hypotheses of brittleness (in the sense given above) and independence are not fulfilled, up to very large scales. Relaxing these initial hypotheses of the weakest-link theory, our statistical physics approach remains statistical by nature and relies on the interplay between internal disorder and stress redistributions. It is based on a mapping of brittle compressive failure onto the critical depinning transition of an elastic manifold, a class of models widely used in non-equilibrium statistical physics characterized by a dynamic phase transition(17). This approach does not consider sample's shape effects(18), only statistical size effects. The critical scaling laws associated to this phase transition naturally predict a saturation of the compressive strength at large scale and are in

remarkable agreement with measurements reported for various materials such as rocks, ice, coal, or concrete.

Compressive failure cannot be captured by a weakest-link approach

Compressive loadings are particularly relevant in rocks mechanics and geophysical situations (19) as the result e.g. of lithostatic pressure, and consequently for geotechnical problems (e.g. (18)). Brittle compressive failure is a complex process, as the local tensile stresses at crack tips are counteracted by the far-field compressive stresses. Consequently, Griffith-like energy balance arguments, or related tools such as fracture toughness, cannot be developed to describe the instability leading to terminal failure, thus making the weakest-link approach inoperative. Instead, brittle compressive failure involves an initiation phase, elastic interactions and stress redistributions, as well as frictional sliding along rough surfaces. In what follows, we mean by brittle failure a situation where microscopic ductile deformation processes such as creep or dislocation motion play a negligible role(20). During the initiation phase, secondary cracks nucleate from the local tensile stresses generated by the frictional sliding along pre-existing defects such as grain boundaries, small joints, or microcracks(21, 22). The propagation of these mode I secondary cracks is however rapidly stopped by the far-field compression. Instead, such nucleation events locally soften the material(23, 24) and thus cause a redistribution of elastic stresses, which in turn can trigger other microcrackings. Then, in the course towards failure, the interaction and linking of secondary cracks is considered to be at the onset of shear fault formation, from which the macroscopic instability is thought to result(22, 25). This process is characterized by a progressive localization of damage and deformation along a fault(26).

The above description shows that all the assumptions of the weakest-link theory are inappropriate in case of compressive failure. Summarizing experimental field and laboratory data obtained for 50 years, it is thus not surprising that their weakest-link predictions are poorly obeyed. When the compressive strength of brittle materials has been measured from laboratory tests over a limited scale range (generally between $\sim 10^{-2}$ m and $\sim 10^{-1}$ m), either non-significant(27, 28) or limited(29, 30) size effects on $\langle \sigma_f \rangle$ were observed, whereas, when reported, the associated variance seemed to increase towards small scales(27). Consequently, these results do not fully constrain empirical or theoretical size effect formulations. Some studies were performed instead several decades ago over a much larger scale range ($\sim 10^{-2}$ m to few m), combining laboratory and in-situ tests(18, 31-33). All of them reported a significant scale-dependence of $\langle \sigma_f \rangle$ at small scales, tentatively and empirically fitted as a

power law decrease(18) $\langle\sigma_f\rangle(L)\sim L^{-\beta}$, but also a non-zero asymptotic strength at large ($> 1\text{m}$) scales, not explained by the weakest link approach. So far, there is no clear explanation for this non-vanishing compressive strength. Instead, empirical formulations of size effects on compressive strength of brittle materials(3, 18, 34) generally ignore such asymptotic behaviour. Following observations at small scales, they all share a common power law scaling $\langle\sigma_f\rangle\sim L^{-\beta}$, with β varying from very small values(29) (i.e. almost no size effect), to the LEFM scaling $\beta=1/2$. The weakest-link concept has been sometimes put forth to explain this scaling for small β values(29), although it is clear from above that this approach is irrelevant in case of compressive failure. On the other hand, a (deterministic) energy analysis of compression failure based on physical (micromechanical) considerations has been proposed(1, 35). In agreement with the scenario described above, it considers that the nucleation of microcracks roughly parallel to the principal compression axis form a band whose mechanical instability, triggered by the buckling of the microslabs separating the microcracks, leads to failure. However, the microcracks, and therefore the associated band, are assumed to nucleate suddenly, just preceding macro-failure. I.e., this approach does not consider the progressive route towards the failure, characterized by elastic interactions between cracks and progressive damage localization. In other words, the transition to failure is considered as a “first-order” transition. This, in addition to an assumed constant scaling between the band length and the size of the system, gives a vanishing strength towards large scales with an asymptotic scaling $\sigma_f\sim L^{-2/5}$, i.e. slightly shallower than the LEFM scaling. Consequently, the observed non-vanishing strength σ_∞ is not explained. In addition, this deterministic approach cannot, by nature, account for a size dependence of the variability of strength. We propose instead to consider compressive failure as a critical transition and develop a mapping onto the depinning transition that allows accounting for the interplay between local disorder and long-ranged elastic interactions leading to a statistical *finite* size effect.

Compressive failure as a critical depinning transition

The modeling of the mechanical behavior of heterogeneous materials induced in recent years an intense research activity. From the early nineties emerged the idea that non-linear processes such as fracture, plasticity and damage could be discussed as critical phenomena (36). In the context of damage, a paradigmatic example of this approach is given by the fiber

bundle model (37). However, the scope of this model as well as its variants (38) are restricted to the catastrophic failure occurring under tensile conditions, i.e. the transition from an initiation stage to a propagating stage triggered by the development of a critical nucleus. In contrast our interest here is the study of progressive damage under compressive conditions. To our knowledge the first attempt of a description of compressive damage as a critical phenomenon is due to Toussaint and Pride(39). They developed a statistical mechanics formalism based on ensemble averages obtained over the rock seen as collection of disordered mesovolumes. A specific Hamiltonian (40) accounted for the interaction between cracks and the traditional tools of equilibrium statistical mechanics (partition function, maximum of entropy) were used to characterize the localization transition associated with the failure of the material.

We here follow a different route. We proposed recently a numerical progressive damage model whose results are consistent with an interpretation of brittle compressive failure as critical phase transition(41, 42). This finite-element model(41) considered a continuous elastic material with progressive local damage: the elastic modulus of an element decreases each time the stress state on that element exceeds a given threshold defined by a Coulomb criterion. This elastic softening simulates an increase in microcrack density at the element scale(23, 24). Disorder was introduced on the local stress threshold. As the result of elastic interactions, the stress redistribution following a damage event can trigger an avalanche of damage. We showed(41, 42) (i) that the size of the largest damage cluster as well as of the largest damage avalanche diverge at peak load, which just precedes failure, and (ii) the divergence of a correlation length ξ at failure, $\xi \sim \Delta^{-1/\nu}$, where $\Delta = \frac{\epsilon_{mf} - \epsilon_m}{\epsilon_{mf}}$ (respectively $\Delta = \frac{\sigma_f - \sigma}{\sigma_f}$) is the control parameter for strain- (respectively stress-) driven simulations, ϵ_m the applied macroscopic strain, ϵ_{mf} the corresponding value at peak stress σ_f (failure), and $\nu = 1.0 \pm 0.1$ the correlation length exponent.

Here, in the spirit of a recent model of amorphous plasticity(43), we formalize this interpretation of compressive failure as a critical transition through a mapping onto a depinning model, a class of models that exhibit out-of-equilibrium phase transition. The damaging process is described as the motion of a d -dimensional elastic manifold with long-range interactions through a random field of obstacles within a space of dimension $d+1$. In our case, the macroscopic stress plays the role of the driving force and a local damage event

corresponds to the depinning from an obstacle, with elastic redistributions in both cases. Damage is represented by a scalar field $D(\mathbf{r})$ at a mesoscopic scale λ , that typically corresponds to the correlation length of the structural disorder of the material, and it occurs whenever the stress state $\boldsymbol{\sigma}$ reaches the boundary of an elastic domain defined by the Coulomb criterion, $|\tau| + \mu\sigma_N = \tau_C$. This criterion is of wide applicability for brittle materials under compressive stress states to define the onset of damage (19, 44). τ and σ_N are respectively the shear and normal stress (sign convention positive in tension) over a plane maximizing the Coulomb stress $|\tau| + \mu\sigma_N$, and $\mu = \tan(\varphi)$ is an internal friction coefficient (φ is the so-called angle of internal friction). The heterogeneous nature of the material, i.e. the disorder, is accounted for by a statistical variability of the cohesion $\tau_C, \delta\tau_C$.

A crucial feature is the non-independence of the local damaging events occurring in the material. Any local event is characterized by a local decrease of the elastic modulus that occurs in a small region surrounded by the remainder of the material. The latter can be seen as an elastic matrix and its reaction induces an elastic stress field all over the material. We started from the classical inhomogeneity problem of Eshelby(45, 46) to calculate the stress field induced by a damaged inclusion. Since the damaged material is elastically disordered, the internal stress cannot be obtained by a simple superposition of the contributions of isolated inclusions. In order to partly account for interactions between inclusions, we develop a two-step strategy to compute the internal stress (see SI). The damage field is first used to obtain a self-consistent estimate of the average, macroscopic elastic behavior, \bar{E} . This effective value, which partly accounts for interactions between inclusions, is then used to obtain a fluctuating damage field, defined from the contrast between the actual elastic moduli at micro-scale and \bar{E} . The internal stress is finally obtained from the sum of the elastic contributions of the associated effective inclusions. The interplay between local disorder and elasticity is the basis for depinning models, which have proved successful in recent years to describe physical and mechanical phenomena as various as the advance or receding of triple contact line on a disordered substrate (47-49), the motion of a magnetic wall in a thin film (50), the propagation of a crack front in a heterogeneous material (51-54), etc. The full derivation of our problem is given in the SI. It allows a complete mapping onto a depinning model, with the following equation of evolution of the damage field:

$$\mu \frac{\partial D}{\partial t}(\mathbf{r}) = \mathcal{R}[\sigma_s^{ext} + \sigma_s^{el}(\{D\}, \bar{E}(\{D\}), \mathbf{r}/\lambda) - 2\cos(\varphi)\tau_C(\mathbf{r}, D)] \quad (1)$$

where \mathcal{R} denotes the positive part, μ is a mobility coefficient and λ is the characteristic length scale of the microstructural disorder. In the language of depinning models, we identify σ_s^{ext} as the external forcing term, σ_s^{el} as the elastic contribution induced by the damage field D , via the knowledge of the damage dependent effective modulus \bar{E} , and τ_c the disorder.

This formal mapping enables us to apply to progressive damage the various analytical and numerical results obtained in the framework of the depinning transition. In the “thermodynamic” limit, i.e. for a system of infinite size, a well-defined critical threshold σ_{th} separates the static phase (limited damage) from the dynamic one (failure). For our problem, this is the expression of a non-vanishing asymptotic strength, $\sigma_\infty > 0$. In case of samples of finite size, fluctuations of the measured threshold σ_f are expected in the vicinity of σ_{th} . We thus expect, as for the threshold force of the depinning transition(6, 55), a finite-size scaling for the compressive strength σ_f of the form:

$$\delta(\sigma_f)(L) = A L^{-1/\nu_{FS}} \quad , \text{ or } \quad \frac{\delta(\sigma_f)(L)}{\sigma_\infty} = \left(\frac{L}{L_A}\right)^{-1/\nu_{FS}} \quad (2)$$

$$\langle \sigma_f \rangle(L) = B L^{-1/\nu_{FS}} + \sigma_\infty \quad , \text{ or } \quad \frac{\langle \sigma_f \rangle(L)}{\sigma_\infty} = \left(\frac{L}{L_B}\right)^{-1/\nu_{FS}} + 1 \quad (3)$$

where ν_{FS} is the finite-size exponent and σ_∞ a non-vanishing asymptotic value of the strength for $L \rightarrow +\infty$. A, B (in $\text{Pa}\cdot\text{m}^{1/\nu_{FS}}$), $L_A = \left(\frac{A}{\sigma_\infty}\right)^{\nu_{FS}}$ and $L_B = \left(\frac{B}{\sigma_\infty}\right)^{\nu_{FS}}$ (in m) are constants. These length scales define the scales below which respectively the fluctuations and the finite-size corrections become important compared to the asymptotic strength σ_∞ . We expect these to scale as $L_{A,B} \sim \lambda \left(\frac{\delta\tau_c}{\tau_c}\right)^{\nu_{FS}}$, where $\frac{\delta\tau_c}{\tau_c}$ represents the associated variability on the local cohesive strength (see S.I.). This implies that in case of weak disorder L_A and L_B will be of the order of λ (e.g. grain size, aggregate size,..), but might be significantly larger in case of strong disorder when e.g. cracks or joints widely distributed in size are initially present in the material. The classical assumption(55) is $\nu = \nu_{FS}$, while the mean-field prediction(56) is $\nu = 1$. Equation (2) expresses the variability on strength intrinsically related to the failure process, on which experimental sources of variability should be added. Towards very small scales, $L \ll \lambda$, the proposed scaling (equations (2) and (3)) necessarily breaks down when σ_f approaches the material strength limit (1).

Application to experimental data in cohesive materials

In full qualitative agreement with experimental data (see above), this finite-size scaling implies an apparent power law decay of the mean strength at small sizes, a non-vanishing strength for $L \rightarrow +\infty$, and an increasing variability towards small sizes. Relation (2) is hardly testable from experimental data, as $\delta(\sigma_f)$ values, when reported, are based on a limited number of independent tests and include experimental-related scatter. For studies including field tests at the meter scale(18, 31-33) and assuming that the asymptotic strength σ_∞ was reached at the largest scale, we fitted the data with relation (3). The agreement is remarkable, with the best-fit ν_{FS} value ranging from 0.8 to 1.05 (Fig. 1), i.e. close to the mean-field prediction, $\nu=1$. The corresponding length scales L_B range from ~ 20 to 40 cm, a possible sign of relatively strong disorder (joints, microcracks) in these natural rock samples. For studies based only on lab tests, either:

- (i) no significant size effect on strength is reported, as for fresh-water granular ice (27), limestone (57), granite (57), or concrete (28). This can be explained by a small L_B in equation (3) and/or an insufficient dataset to properly sample size effects;
- (ii) or the data can be well fitted by (3) assuming $\nu_{FS}=1$, as shown on figure S1 for high-performance (HP) concrete (30) and marble (29). In case of HP concrete, the scale L_B is close to the maximum size of the andesite aggregate (12 mm) (30). In agreement with our former expectation, in such initially unfractured materials, the microstructural scale (aggregate size, grain size, ..) likely sets this L_B scale.

The confining pressure σ_3 increases the axial compressive strength σ_{1f} of rocks, ice, coal or concrete (19, 28, 34, 58). Up to a confining ratio σ_3/σ_{1f} of about 30%, failure is brittle and occurs through microcrack initiation and interactions, followed by shear fault formation at the onset of macroscopic instability, as described above(58). This failure mode is sometimes called Coulombic faulting, reminiscent of the importance of solid friction in this case(44). Consequently, one expects our mapping to the depinning transition to hold in this case. The combination of the effects of size and of confining pressure on strength has been rarely studied, but the available data on coal (34) are well explained by equation (2) with $\nu_{FS}=1$ and an increasing asymptotic strength σ_∞ with increasing confinement, as expected (Figure 2). For these natural samples, the scale L_B is once again relatively large (several cm). It slightly decreases with increasing confinement, suggesting a secondary effect of confinement on the sensibility of L_B to the variability of the local strength, $\frac{\delta\tau_c}{\tau_c}$. For such multiaxial compression tests, the deviatoric stress $\sigma_1 - \sigma_3$ appears as the most relevant variable. Thus, the strength

has been defined as $\sigma_f = \sigma_{1f} - \sigma_3$. This choice for σ_f , instead of the axial strength σ_{1f} , obviously doesn't change the value of the exponent ν_{FS} or of the scale L_B . For confinements larger than $\sim 30\%$, compressive failure is no more brittle, and another failure mode occurs, as mode I secondary crack nucleation is inhibited. This failure mode, called plastic faulting, involves thermal softening and an adiabatic shear instability (59). In this case, we no longer expect elastic interactions between microcracks to occur, i.e. our size effect formalism to hold. Indeed, it has been found that for large confining pressure, size effects on compressive strength disappear (60). This sets the range of applicability of our formalism.

Application to granular media

This mapping onto the depinning problem is likely not restricted to brittle cohesive materials. As described in (43) and recalled in the SI, it can be extended to the macroscopic plastic instability in amorphous media. The case of a cohesionless frictional granular medium compressed under confinement can be interpreted as an intermediate case between amorphous plasticity and compressive damage. Indeed, shear-induced local rearrangements of the granular structure lead to irreversible local strains but not to a systematic degradation of local stiffness. Compared to amorphous plasticity, other complications are present, however, such as dilatancy. When compressed under confinement, these media exhibit a macroscopic flowing instability associated to strain localization(61), which sets the yield stress, i.e. the “strength”. This instability can also be considered as a critical transition(62). In this case, the disorder is topological, coming from the arrangement of particles.

From this analogy, we expect finite-size scaling (relations (2) and (3)) to ensue. However, to our knowledge, there is so far no experimental data over a significant range of scales to check this anticipation. We therefore simulated the mechanical behaviour of frictional granular materials using the Molecular Dynamics discrete element method (63). Two-dimensional granular assemblies made of a set of frictional circular grains were considered. The dynamic equations were solved for each grain, which interact via linear elastic laws and Coulomb friction when they are in contact (64). Neither cohesion between grains, nor rolling resistance were considered. In order to build granular assemblies with strongly different initial (before loading) characteristics, in terms of coordination number and/or packing density, specific sample preparation procedures were used. Details on the discrete element model as well as on these procedures are given in the SI. These granular assemblies were loaded under a multi-

axial configuration, with the external axial stress σ_1 prescribed in order to impose a constant axial strain-rate, whereas the radial stress σ_3 , i.e. the confining pressure, was kept constant. The 2D sample sizes varied from 100 to ~ 45000 grains.

Whatever the initial characteristics of the assemblies, finite size scaling of compressive strength was observed, in full agreement with equations (2) and (3) (Fig. 3), showing the generic nature of the concept proposed here. In agreement with our expectation, the scales L_A and L_B were slightly larger than the average particle size, and increased for less dense, less coordinated samples.

Failure strength statistics

As noted in the introduction, the weakest-link hypothesis leads to extreme value statistics for the probability of failure under an applied stress σ . As the weakest-link theory appears irrelevant for compressive failure, we do not expect such extreme statistics for the distribution of strength in this case. Published experimental data with a sufficient number of failure tests to analyze strength distributions are rare. Results obtained on ice indeed exclude extreme statistics, either Weibull or Gumbel, and argue instead for Gaussian statistics (Fig. 4). The same is true for the discrete-element modeling of frictional granular media (Fig. S2). We anticipate, from the criticality of the transition, the scaling form of the distribution $P(\sigma_f, L)$ of the fluctuations for a system of size L as $P(\sigma_f, L) = L^{\nu_{FS}} \Psi[(\sigma_{th} - \sigma_f)L^{\nu_{FS}}]$. Such a scaling form naturally leads to the scaling relations for the mean value $\langle \sigma_f \rangle$ (relation (3)) and the standard deviation $\delta(\sigma_f)$ (relation (2)) of the compressive strength discussed above. However, the precise form of the statistical distribution Ψ is not prescribed by this simple scaling analysis. In particular, Ψ is not expected to obey the predictions of extreme value statistics whose hypotheses (absence of interactions) are not satisfied in the present problem. In recent results obtained in a similar framework (depinning model of amorphous plasticity (65)), Gaussian-like distributions were observed as well.

Combining Gaussian statistics with equations (2) and (3) leads to the following expression for the probability of failure at scale L under a stress σ :

$$P_F(\sigma, L) = \frac{1}{2} \left[1 + \operatorname{erf} \left(\frac{\sigma - \sigma_\infty \left(1 + \left(\frac{L}{L_B} \right)^{-1/\nu_{FS}} \right)}{\sqrt{2} \sigma_\infty \left(\frac{L}{L_A} \right)^{-1/\nu_{FS}}} \right) \right] \quad (4)$$

Concluding comments

This new, statistical physics interpretation of compressive failure of continuous and granular media has important practical consequences. First, when lab-scales (cm to dm) studies show no significant size effect, one expects that lab strength values give a good estimate of the asymptotic (field) strength. Extrapolation of lab-scales data to scales smaller than L_A or L_B will be more difficult, owing to the intrinsic variability at such scales. However, the mean-field estimate of the finite-size exponent, $\nu_{FS}=1$, obtained from theoretical considerations, well describes the fluctuations and the associated finite-size corrections, whereas for initially unfractured materials, L_A and L_B are related to the characteristic microstructural scale (grain size, aggregate size, ..). Therefore, owing to its predictive potential, we believe that the proposed scaling is a useful, simple to use guidance for future structural design rules or regulations (e.g. (2)).

Materials and Methods

The characteristics and the simulation settings of the discrete-element model of frictional granular media are given in the *Supporting Information*, along with the formal derivation of the mapping of brittle compressive failure onto the depinning transition of an elastic manifold.

Acknowledgments

All numerical simulations were performed at SCCI-CIMENT Grenoble. J.W. and D.V. acknowledge the hospitality of the Aspen Center for Physics, which is supported by the National Science Foundation Grant No. PHY-1066293, as the seminal ideas of this work came up during their stay at the Center. S. Zapperi and D. Bonamy are acknowledged for interesting discussions and suggestions.

References

1. Bazant ZP & Planas J (1998) *Fracture and size effect in concrete and other quasibrittle materials* (CRC Press, Boca Raton).

2. Standardization ECf (2002) Eurocode 2: Design of Concrete Structures - Part 1-1: General rules and rules for buildings, EN 1995-1-1.
3. Heuze FE (1980) Scale effects in the determination of rock mass strength and deformability. *Rock Mechanics* 12:167-192.
4. Mariotte E (1686) *Traité du mouvement des eaux et des autres corps fluides* (Paris).
5. Bazant ZP (2004) Scaling theory for quasibrittle structural failure. *Proceedings of the National Academy of Sciences of the United States of America* 101(37):13400-13407.
6. Zapperi S (2012) Current challenges for statistical physics in fracture and plasticity. *Eur. Phys. J. B* 85:329.
7. Weibull W (1939) A statistical theory of the strength of materials. *Proc. Royal Swedish Academy of Eng. Sci.* 151:1-45.
8. Gumbel EJ (1958) *Statistics of extremes* (Columbia University Press, New York).
9. Fisher RA & Tippett LHC (1928) Limiting forms of the frequency distribution of the largest or smallest members of a sample. *Math. Proc. Cambridge Philos. Soc.* 24:180-190.
10. Weibull W (1951) A statistical distribution function of wide applicability. *J. Applied Mechanics* 18:293-297.
11. Alava MJ, Nukala P, & Zapperi S (2009) Size effects in statistical fracture. *J. Phys. D-Appl. Phys.* 42(21).
12. Sornette D (2000) *Critical phenomena in natural sciences* (Springer, Berlin).
13. Beremin FM (1983) A local criterion for cleavage fracture of a nuclear pressure vessel steel. *Metallurgical Transactions A* 14A:2277-2287.
14. Miannay D (1998) *Fracture Mechanics* (Springer, Berlin).
15. Bazant ZP (1984) SIZE EFFECT IN BLUNT FRACTURE - CONCRETE, ROCK, METAL. *Journal of Engineering Mechanics-Asce* 110(4):518-535.
16. Alava MJ, Nukala PKV, & Zapperi S (2006) Statistical models of fracture. *Advances in Physics* 55(3-4):349-476.
17. Fisher DS (1998) Collective transport in random media: from superconductors to earthquakes. *Physics Reports* 301:113-150.
18. Hustrulid WA (1976) A review of coal pillar strength formulas. *Rock Mechanics* 8:115-145.
19. Jaeger JC & Cook NGW (1979) *Fundamentals of Rock Mechanics* (Chapman and Hall, London).
20. Schulson EM (2001) Brittle failure of ice. *Engineering Fracture Mechanics* 68(17-18):1839-1887.
21. Nemat-Nasser S & Horii H (1982) Compression-induced nonplanar crack extension with application to splitting, exfoliation, and rockburst. *J. Geophys. Res.* 87:6805-6821.
22. Schulson EM, Iliescu D, & Renshaw C (1999) On the initiation of shear faults during brittle compressive failure: a new mechanism. *J. Geophys. Res.* 104:695-705.
23. Kachanov M (1994) Elastic solids with many cracks and related problems. *Advances in applied mechanics* 30:259-445.
24. Cox SJD & Meredith PG (1993) MICROCRACK FORMATION AND MATERIAL SOFTENING IN ROCK MEASURED BY MONITORING ACOUSTIC EMISSIONS. *International Journal of Rock Mechanics and Mining Sciences & Geomechanics Abstracts* 30(1):11-24.
25. Katz O & Reches Z (2004) Microfracturing, damage, and failure of brittle granites. *J. Geophys. Res.-Solid Earth* 109(B1).
26. Lockner DA, Byerlee JD, Kuksenko V, Ponomarev A, & Sidorin A (1991) Quasi-static fault growth and shear fracture energy in granite. *Nature* 350:39-42.
27. Kuehn GA, Schulson EM, Jones DE, & Zhang J (1992) The compressive strength of ice cubes of different sizes. in *OMAE* (ASME), pp 349-356.
28. van Mier JGM (1986) Multiaxial strain-softening of concrete, Part I: Fracture. *Materials and Structures* 19:179-190.
29. Mogi K (1962) The influence of the dimensions of specimens on the fracture strength of rocks. *Bull. Earthquake Res. Inst.* 40:175-185.

30. del Viso JR, Carmona JR, & Ruiz G (2008) Shape and size effects on the compressive strength of high-strength concrete. *Cement and Concrete Research* 38:386-395.
31. Pratt HR, Black AD, Brown WS, & Brace WF (1972) The effect of specimen size on the mechanical properties of unjointed diorite. *Int. J. Rock Mech. Min. Sci.* 9:513-529.
32. Bieniawski ZT (1968) The effect of specimen size on compressive strength of coal. *Int. J. Rock Mech. Min; Sci.* 5(4):325-335.
33. Brace WF (1981) The effect of size on mechanical properties of rock. *Geophys. Res. Lett.* 8(7):651-652.
34. Hoek E & Brown ET (1997) Practical estimates of rock mass strength. *Int. J. Rock Mech. Min. Sci.* 34(8):1165-1186.
35. Bazant ZP & Xiang Y (1994) Compression failure of quasibrittle materials and size effect. *Damage Mechanics in Composites - ASME Winter Annual Meeting*, eds Allen DH & Ju JW (AMD), pp 143-148.
36. Herrmann HJ & Roux S (1990) *Statistical models for the fracture of disordered media* (North-Holland, Amsterdam).
37. Pradhan S, Hansen A, & Chakrabarti BK (2010) Failure processes in elastic fiber bundles. *Rev. Mod. Phys.* 82(1):499-555.
38. Delaplace A, Roux S, & Pijaudier-Cabot G (1999) 'Damage cascade' in a softening interface. *International Journal of Solids and Structures* 36(10):1403-1426.
39. Toussaint R & Pride SR (2002) Fracture of disordered solids in compression as a critical phenomenon. I. Statistical mechanics formalism. *Phys. Rev. E* 66(3).
40. Toussaint R & Pride SR (2002) Fracture of disordered solids in compression as a critical phenomenon. II. Model Hamiltonian for a population of interacting cracks. *Phys. Rev. E* 66(3).
41. Girard L, Amitrano D, & Weiss J (2010) Fracture as a critical phenomenon in a progressive damage model. *J. Stat. Mech.* P01013.
42. Girard L, Weiss J, & Amitrano D (2012) Damage-cluster distributions and size effect on strength in compressive failure. *Phys. Rev. Lett.* 108:225502.
43. Talamali M, Petäjä V, Vandembroucq D, & Roux S (2012) Strain localization and anisotropic correlations in a mesoscopic model of amorphous plasticity. *Comptes Rendus Mecanique* 340(4-5):275-288.
44. Weiss J & Schulson EM (2009) Coulombic faulting from the grain scale to the geophysical scale: Lessons from ice. *J. Phys. D: Appl. Phys.* 42:214017.
45. Eshelby JD (1957) The determination of the elastic field of an ellipsoidal inclusion, and related problems. *Proc. Roy. Soc. A* 241:376.
46. Eshelby JD (1959) Elastic field of an ellipsoidal inclusion *Proc. Roy. Soc. A* 252:561.
47. Joanny JF & Degennes PG (1984) A MODEL FOR CONTACT-ANGLE HYSTERESIS. *Journal of Chemical Physics* 81(1):552-562.
48. Moulinet S, Rosso A, Krauth W, & Rolley E (2004) Width distribution of contact lines on a disordered substrate. *Phys. Rev. E* 69(3).
49. Bonn D, Eggers J, Indekeu J, Meunier J, & Rolley E (2009) Wetting and spreading. *Rev. Mod. Phys.* 81(2):739-805.
50. Lemerle S, *et al.* (1998) Domain wall creep in an Ising ultrathin magnetic film. *Phys. Rev. Lett.* 80(4):849-852.
51. Gao HJ & Rice JR (1989) A First-Order Perturbation Analysis of Crack Trapping by Arrays of Obstacles. *Journal of Applied Mechanics-Transactions of the Asme* 56(4):828-836.
52. Santucci S, *et al.* (2007) Statistics of fracture surfaces. *Phys. Rev. E* 75(1).
53. Dalmas D, Lelarge A, & Vandembroucq D (2008) Crack Propagation through Phase-Separated Glasses: Effect of the Characteristic Size of Disorder. *Phys. Rev. Lett.* 101(25).
54. Bonamy D & Bouchaud E (2011) Failure of heterogeneous materials: A dynamic phase transition? *Phys. Rep.-Rev. Sec. Phys. Lett.* 498(1):1-44.
55. Narayan O & Fisher DS (1993) Threshold critical dynamics of driven interfaces in random media. *Phys. Rev. B* 48(10):7030-7042.

56. Ertas D & Kardar M (1994) Critical dynamics of contact line depinning. *Phys. Rev. E* 49(4):R2532-R2535.
57. Thuro K, Plinninger RJ, Zäh S, & Schütz S (2001) Scale effects in rock strength properties. Part I: unconfined compressive test and Brazilian test. *EUROCK 2001: Rock Mechanics - A Challenge for Society*, ed Eloranta Sa (Swets & Zeitlinger Lisse), pp 169-174.
58. Renshaw CE & Schulson EM (2001) Universal behavior in compressive failure of brittle materials. *Nature* 412:897-900.
59. Renshaw CE & Schulson EM (2004) Plastic faulting: Brittle-like failure under high confinement. *J. Geophys. Res.* 109:B09207.
60. Habib P & Vouille G (1966) Sur la disparition de l'effet d'échelle aux hautes pressions. *Comptes Rendus hebd. Séanc. Acad. Sci. Paris* 262:715-717.
61. Desrues J & Viggiani G (2004) Strain localization in sand: an overview of the experimental results obtained in Grenoble using stereophotogrammetry. *Int. J. Numer. Anal. Methods Geomech.* 28(4):279-321.
62. Gimbert F, Amitrano D, & Weiss J (2013) Crossover from quasi-static to dense flow regime in compressed frictional granular media. *EPL* 104:46001.
63. Radjai F & Dubois F (2011) *Discrete-element modelling of granular materials* (Wiley).
64. Agnolin I & Roux JN (2007) Internal states of model isotropic granular packings. I. Assembling process, geometry, and contact networks. *Phys. Rev. E* 76(6).
65. Talamali M, Petäjä V, Vandembroucq D, & Roux S (2011) Avalanches, precursors, and finite-size fluctuations in a mesoscopic model of amorphous plasticity. *Phys. Rev. E* 84(1).

Figures

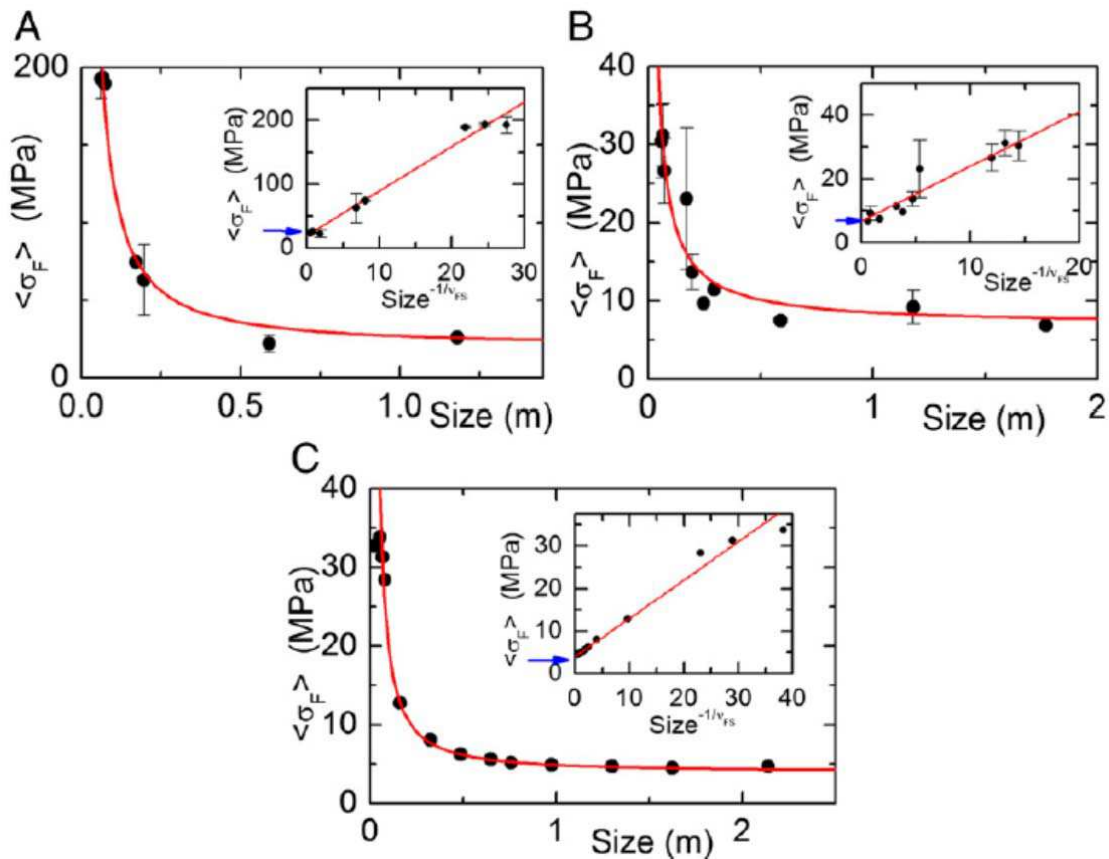


Figure 1. Finite-size effect on uniaxial compressive strength (experimental data). (a) Granodiorite(31), (b) Quartz diorite(31), (c) Coal(32). Main graphs: Mean compressive strength $\langle\sigma_f\rangle$ vs size. Black circles: published experimental data, with associated standard deviation (when reported). Red curve: fit by equation (3), using $\sigma_\infty=20$ MPa for granodiorite, 6.8 MPa for quartz diorite, and 4 MPa for coal. The best-fit ν_{FS} exponents are respectively 0.85, 1.05 and 0.8. The associated constants length scales L_B are respectively 0.41, 0.235 and 0.30 m. Insets: Same data and fits, in a $\langle\sigma_f\rangle$ vs $L^{-1/\nu_{FS}}$ graph where equation (3) is as straight line and that reveals the asymptotic strength σ_∞ .

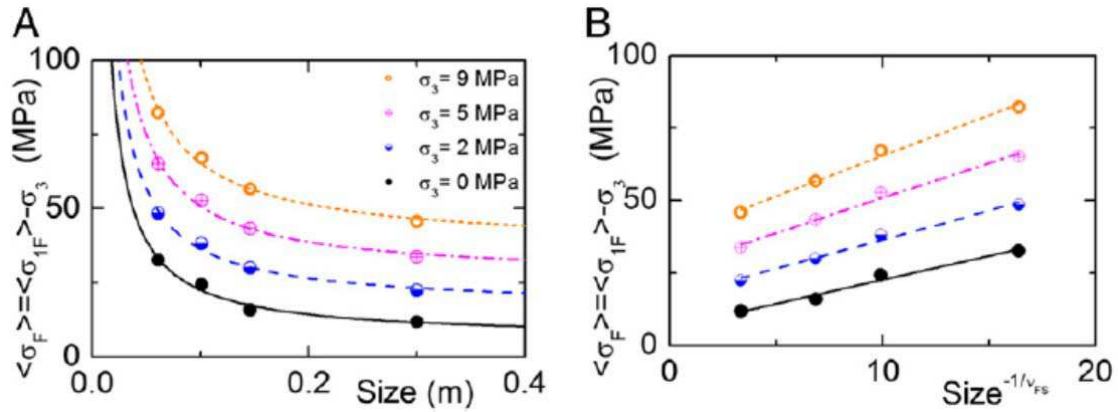


Figure 2. Finite-size effect on multiaxial compressive strength for coal (experimental data). These strength values have been recalculated using the generalized Hoek and Brown empirical formulation (equation (1) of Ref(34)) and using the set of parameters found in table 3 of the same Ref., for confining pressure $\sigma_3=0, 2, 5$ and 9 MPa. (a): Mean compressive strength $\langle\sigma_f\rangle = \langle\sigma_{1f}\rangle - \sigma_3$ vs size. For this multiaxial loading, the deviatoric stress has been considered here as the relevant variable. The corresponding fits from equation (3) of the main text, using $\nu_{FS}=1$, are shown as lines. The best-fit asymptotic strengths σ_∞ are respectively 6.1, 16.6, 26.9 and 37.4 MPa for $\sigma_3=0, 2, 5$ and 9 MPa. The associated L_B values are respectively 27, 12, 9 and 7.5 cm. (b) Same data and fits, in a $\langle\sigma_f\rangle$ vs $L^{-1/\nu_{FS}}$ graph where equation (3) is as straight line and that reveals the asymptotic strength σ_∞ .

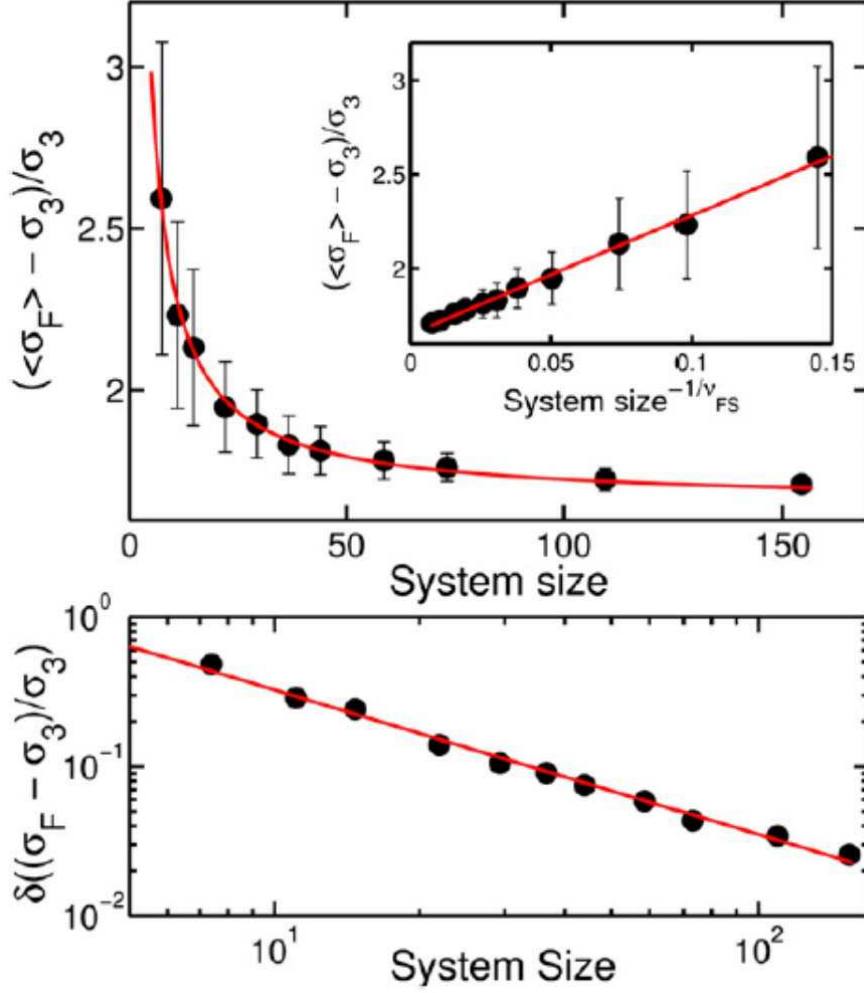


Figure 3. Finite size effects for the discrete-element model of frictional granular media under multiaxial compression (LC1 samples; see SI for details about the model), and then normalized by the confining pressure σ_3 . (top) Mean compressive strength $\frac{\langle \sigma_f \rangle}{\sigma_3} = \frac{\langle \sigma_{1f} \rangle - \sigma_3}{\sigma_3}$ and (bottom) associated standard deviation vs system size. System size has been defined as $\sqrt{N_g}$, where N_g is the number of grains of the model. Black circles: model results. Red curves: finite size scaling given by equation (3) for the mean strength and equation (2) for the standard deviation, with $\nu_{FS}=1.07$, $L_A=1.68$, $L_B=4.21$ and $\sigma_\infty=1.65 \times \sigma_3$. The best-fit exponent ν_{FS} and scale L_A were obtained from the standard deviation scaling (bottom), the asymptotic strength σ_∞ and scale L_B were then obtained from the scaling of $\frac{\langle \sigma_f \rangle}{\sigma_3}$ (inset of (top)). Inset of (top): Same data and fits, in a $\frac{\langle \sigma_f \rangle}{\sigma_3}$ vs $L^{-1/\nu_{FS}}$ graph where equation (3) is as straight line and that reveals the asymptotic strength σ_∞ .

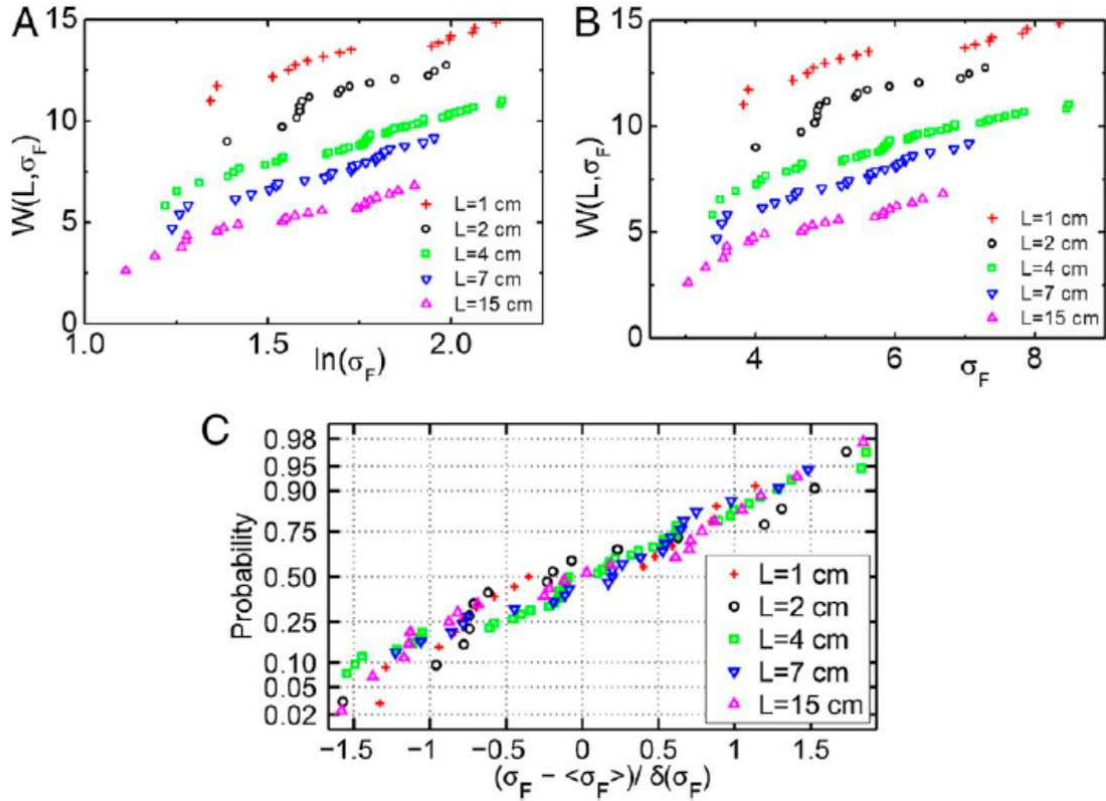


Figure 4. Distribution of uniaxial compressive failure strength for fresh-water granular ice (grain size: ~ 1 mm), from Ref.(27). (a) Weibull statistics, where $W(L, \sigma_f) = \ln\left(\frac{-\ln(1-P_F(\sigma))}{L^3}\right)$ and $P_F(\sigma)$ is the (cumulative) probability of failure under an applied stress σ . Since data obtained for different sample sizes do not collapse onto a single straight line, compressive strengths do not follow Weibull statistics. The same is true for Gumbel statistics (b). (c) Normal probability plot for the standard distributions. The collapse onto a single straight line, which corresponds to equation (4), argues for Gaussian statistics.